

VERY METAL-POOR OUTER-HALO STARS WITH ROUND ORBITS

KOHEI HATTORI¹, YUZURU YOSHII¹, TIMOTHY C. BEERS^{2,3}, DANIELA CAROLLO^{4,5}, AND YOUNG SUN LEE⁶

Draft version December 19, 2012

ABSTRACT

The orbital motions of halo stars in the Milky Way reflect the orbital motions of the progenitor systems in which they formed, making it possible to trace the mass-assembly history of the Galaxy. Direct measurement of three-dimensional velocities, based on accurate proper motions and line-of-sight velocities, has revealed that the majority of halo stars in the inner-halo region move on eccentric orbits. However, our understanding of the motions of distant, in-situ halo-star samples is still limited, due to the lack of accurate proper motions for these stars. Here we explore a model-independent analysis of the line-of-sight velocities and spatial distribution of a recent sample of 1865 carefully selected halo blue horizontal-branch (BHB) stars within 30 kpc of the Galactic center. We find that the mean rotational velocity of the very metal-poor ($[\text{Fe}/\text{H}] < -2.0$) BHB stars significantly lags behind that of the relatively more metal-rich ($[\text{Fe}/\text{H}] > -2.0$) BHB stars. We also find that the relatively more metal-rich BHB stars are dominated by stars with eccentric orbits, as previously observed for other stellar samples in the inner-halo region. By contrast, the very metal-poor BHB stars are dominated by stars on rounder, lower-eccentricity orbits. Our results indicate that the motion of the progenitor systems of the Milky Way that contributed to the stellar populations found within 30 kpc correlates directly with their metal abundance, which may be related to their physical properties such as gas fractions. These results are consistent with the existence of an inner/outer halo structure for the halo system, as advocated by Carollo et al.

Subject headings: Galaxy: evolution — Galaxy: formation — Galaxy: halo — Galaxy: kinematics and dynamics

1. INTRODUCTION

The luminosity of the Milky Way is dominated by its disk, where the great majority of stars ($> 90\%$) are found. By comparison, out of $\sim 10^{11}$ stars in the Milky Way, the stellar halo comprises only a tiny fraction ($\sim 1\%$), but this component is a precious source of information on the formation history of the Galaxy. First, halo stars are very old ($\sim 10\text{--}13$ Gyrs), and their chemical compositions provide information on the ancient environments in which these stars formed. Typically, the metal abundances of halo stars are less than 1/10th of the Solar value (Chiba & Beers 2000; Carollo et al. 2007, 2010), which immediately suggests that the metal enrichment due to supernova explosions in the Universe had not progressed very far when halo stars were formed. Secondly, the stellar halo is a collisionless system, hence two-body relaxation is expected to be unable to fully erase the initial orbital properties of halo stars. It follows that the present motions of halo stars reflects their motions in the early Universe, which can be used to explore the kinematics of their progenitor systems, such as the gas clouds or dwarf galaxies in which these halo stars formed.

To date, detailed analyses of the chemical and dynamical properties of halo stars has been confined to stars up to $\sim 10\text{--}15$ kpc from the Sun (centered at the Galactocentric

distance of the Sun, ~ 8.5 kpc), although the spatial distribution of the stellar halo extends to ~ 100 kpc or more. This is mainly because we do not possess sufficiently accurate measurements of proper motions for more distant halo stars. In order to avoid this limitation, many authors have studied the line-of-sight velocities and spatial distribution of halo stars, making use of various kinematic models – such as distribution function models of the stellar halo, or gravitational potential models of the Milky Way. However, the conclusions of previous studies on the orbital distribution of halo stars well outside the local region are divergent. Some suggest tangentially-anisotropic orbital distributions (Sommer-Larsen et al. 1997; Kafle et al. 2012), others suggest radially-anisotropic distributions (Deason et al. 2012), and still others suggest nearly isotropic distributions (Sirko et al. 2004; Thom et al. 2005). This might imply that the stellar halo is not a simple entity which can be described by a single distribution function model. Indeed, based on observations of relative nearby ($d \leq 4$ kpc) halo stars, (Carollo et al. 2007, 2010) suggest that a dual-halo model is more appropriate, in which the stellar halo consists of a relatively metal-rich inner-halo component with a net zero to slightly prograde rotation, and a very metal-poor outer-halo component with a net retrograde rotation. Recent observations of retrograde outer-halo RR Lyrae stars by Kinman et al. (2012), and a model-fitting analysis for distant halo stars by Deason et al. (2011) supports this idea, as do recent numerical simulations of the formation of Milky Way-like galaxies (e.g., McCarthy et al. 2012). Here we introduce a new analysis of the halo system, which requires only a minimum of assumptions, and does not require any kinematic models.

This paper is outlined as follows. In Section 2 we describe our sample selection and expected errors in distance, line-of-sight velocities, and metallicities. Section 3 describes our analysis approach. In Section 4, we examine the application

khattori@ioa.s.u-tokyo.ac.jp

¹ Institute of Astronomy, School of Science, University of Tokyo, 2-21-1, Osawa, Mitaka, Tokyo 181-0015, Japan

² National Optical Astronomy Observatories, Tucson, AZ 85719, USA

³ Department of Physics & Astronomy and JINA: Joint Institute for Nuclear Astrophysics, Michigan State University, E. Lansing, MI 48824, USA

⁴ Macquarie University - Dept. Physics & Astronomy, Sydney, 2109 NSW, Australia

⁵ INAF - Osservatorio Astronomico di Torino, 10025 Pino Torinese, Torino - Italy

⁶ Department of Astronomy, New Mexico State University, Las Cruces, NM 88003, USA

of this technique to our sample of halo BHB stars, segregated on metallicity. Section 5 presents a brief discussion and conclusions.

2. SAMPLE SELECTION

Our sample comprises 1865 blue horizontal-branch (BHB) stars from Data Release 8 of the Sloan Digital Sky Survey (Aihara et al. 2011), with Galactocentric distances in the range $6 < r/\text{kpc} < 30$, as originally selected and carefully validated by Xue et al. (2011). This sample is free from significant contamination by the Sagittarius stream and the thick disk, as we apply a spatial masking scheme in their selection. Distances from the Sun are accurate to $\sim 5 - 10\%$, and the line-of-sight velocity errors are $5 - 20 \text{ km s}^{-1}$ (see Xue et al. 2011). Stellar metallicities, $[\text{Fe}/\text{H}]$, for this sample are also available. Following Xue et al. (2011), we use the metallicities obtained by the Wilhelm et al. methodology in the SEGUE Stellar Parameter Pipeline (SSPP; see Lee et al. 2008 for details), which are likely to be the most reliable for stars with effective temperatures of BHB stars (on the order of 0.3 dex). We then divide this sample on metallicity – 994 of our stars are relatively metal-rich ($[\text{Fe}/\text{H}] > -2.0$), while 871 stars are very metal-poor ($[\text{Fe}/\text{H}] < -2.0$).⁷

3. ANALYSIS METHOD

3.1. Derivation of Rotational Velocity

Let us denote by S an imaginary observer located at the Sun who is at rest with respect to the Galactic rest frame, and by O an observer located at the Sun who moves with the Sun. Here, we assume that the velocity of O with respect to S , \mathbf{v}_\odot , and the three-dimensional (3D) position of the Sun with respect to the Galactic center are known.

Now, suppose that the k -th star ($k = 1, \dots, n$) is observed in the direction of $\mathbf{x}_k^{\text{los}}$ by S and O . Then, the line-of-sight velocity with respect to S can be expressed as:

$$v_k^{\text{los}} \equiv \mathbf{v}_k \cdot \mathbf{x}_k^{\text{los}}, \quad (1)$$

where \mathbf{v}_k is the velocity of this star with respect to S . Since the line-of-sight velocity of this star with respect to O is:

$$v_k^{\text{los, hel}} \equiv (\mathbf{v}_k - \mathbf{v}_\odot) \cdot \mathbf{x}_k^{\text{los}} = v_k^{\text{los}} - \mathbf{v}_\odot \cdot \mathbf{x}_k^{\text{los}}, \quad (2)$$

we can calculate v_k^{los} from $(\mathbf{v}_\odot, v_k^{\text{los, hel}}, \mathbf{x}_k^{\text{los}})$.

On the other hand, if we decompose \mathbf{v}_k as:

$$\mathbf{v}_k = v_{r,k} \mathbf{e}_{r,k} + v_{\theta,k} \mathbf{e}_{\theta,k} + v_{\phi,k} \mathbf{e}_{\phi,k}, \quad (3)$$

we obtain

$$v_k^{\text{los}} = v_{r,k} Q_{r,k} + v_{\theta,k} Q_{\theta,k} + v_{\phi,k} Q_{\phi,k}, \quad (4)$$

where

$$Q_{i,k} \equiv \mathbf{x}_k^{\text{los}} \cdot \mathbf{e}_{i,k} \quad (i = r, \theta, \phi). \quad (5)$$

Here, $v_{i,k}$ and $\mathbf{e}_{i,k}$ ($i = r, \theta, \phi$) are the i -th velocity component of the k -th star, and the basis unit vectors of the spherical coordinate system at the position of the k -th star, respectively.

Given the assumptions:

- (A1) There is no correlation between the velocity and position of a star
- (A2) The distributions of v_r , v_θ , and v_ϕ are symmetric around $v_r = 0$, $v_\theta = 0$, and $v_\phi = V_{\text{rot}}$, respectively

then the data points $\{(Q_{\phi,k}, v_k^{\text{los}})\}$ are likely to be distributed around a linear function of form:

$$v^{\text{los}} = V_{\text{rot}} Q_\phi \quad (6)$$

Thus, by performing a linear fit to the data in the $Q_\phi - v^{\text{los}}$ plane, we can obtain \hat{V}_{rot} – by which we denote the estimated value of V_{rot} – by measuring the slope of the best-fit linear function. This approach is similar to that of Frenk & White (1980).

3.2. Derivation of 3D Velocity Dispersion

In estimating the velocity dispersion, we use a modified version of the approach used by Woolley (1978). In principle, this method utilizes the direction dependence of the line-of-sight velocity dispersion.

In addition to (A1) and (A2) above, let us further assume that the velocity distribution of the sample stars satisfies the following:

- (A3) The velocity ellipsoid is aligned with a spherical coordinate system
- (A4) The dispersions in the distributions of v_r , v_θ , and v_ϕ around their centers are σ_r , σ_θ , and σ_ϕ , respectively

Then, it can be shown, for $i = r, \theta, \phi$ (see Morrison et al. 1990 for the case of $i = \phi$), that

$$\begin{aligned} & E[\text{var}[v^{\text{los}} Q_i]] \\ &= \sigma_r^2 \frac{1}{n} \sum_{k=1}^n Q_{i,k}^2 Q_{r,k}^2 + \sigma_\theta^2 \frac{1}{n} \sum_{k=1}^n Q_{i,k}^2 Q_{\theta,k}^2 + \sigma_\phi^2 \frac{1}{n} \sum_{k=1}^n Q_{i,k}^2 Q_{\phi,k}^2 \\ &+ \frac{V_{\text{rot}}^2}{n-1} \left\{ \sum_{k=1}^n Q_{i,k}^2 Q_{\phi,k}^2 - \frac{1}{n} \left(\sum_{k=1}^n Q_{i,k} Q_{\phi,k} \right)^2 \right\}, \quad (7) \end{aligned}$$

where we denote the expectation and variance of X by $E[X]$ and $\text{var}[X]$, respectively.

Thus, by substituting the observed $(\text{var}[v^{\text{los}} Q_i])$ for $E[\text{var}[v^{\text{los}} Q_i]]$, and the already estimated \hat{V}_{rot} for V_{rot} , we obtain:

$$\begin{aligned} & \begin{bmatrix} \text{var}[v^{\text{los}} Q_r] \\ \text{var}[v^{\text{los}} Q_\theta] \\ \text{var}[v^{\text{los}} Q_\phi] \end{bmatrix} - \frac{\hat{V}_{\text{rot}}^2}{n-1} \begin{bmatrix} \sum_k Q_{r,k}^2 Q_{\phi,k}^2 - \frac{1}{n} (\sum_k Q_{r,k} Q_{\phi,k})^2 \\ \sum_k Q_{\theta,k}^2 Q_{\phi,k}^2 - \frac{1}{n} (\sum_k Q_{\theta,k} Q_{\phi,k})^2 \\ \sum_k Q_{\phi,k}^4 - \frac{1}{n} (\sum_k Q_{\phi,k}^2)^2 \end{bmatrix} \\ &= \frac{1}{n} \begin{bmatrix} \sum_k Q_{r,k}^4 & \sum_k Q_{r,k}^2 Q_{\theta,k}^2 & \sum_k Q_{r,k}^2 Q_{\phi,k}^2 \\ \sum_k Q_{r,k}^2 Q_{\theta,k}^2 & \sum_k Q_{\theta,k}^4 & \sum_k Q_{\theta,k}^2 Q_{\phi,k}^2 \\ \sum_k Q_{r,k}^2 Q_{\phi,k}^2 & \sum_k Q_{\theta,k}^2 Q_{\phi,k}^2 & \sum_k Q_{\phi,k}^4 \end{bmatrix} \begin{bmatrix} \hat{\sigma}_r^2 \\ \hat{\sigma}_\theta^2 \\ \hat{\sigma}_\phi^2 \end{bmatrix}. \quad (8) \end{aligned}$$

The solutions $(\hat{\sigma}_r^2, \hat{\sigma}_\theta^2, \hat{\sigma}_\phi^2)$ for this equation are the unbiased estimates for $(\sigma_r^2, \sigma_\theta^2, \sigma_\phi^2)$. Note that these estimated values are not guaranteed to take on positive values, so that we have to confirm the robustness of our method via an independent Monte Carlo simulation, as described below.

⁷ Our boundary metallicity ($[\text{Fe}/\text{H}] = -2.0$) lies between the peak metallicities of the inner-halo ($[\text{Fe}/\text{H}]_{\text{peak}} \simeq -1.6$) and outer-halo ($[\text{Fe}/\text{H}]_{\text{peak}} \simeq -2.2$) components (Carollo et al. 2007).

3.3. Testing the Reliability of our Method

In order to estimate the error that accompanies our estimate of the three-dimensional velocity dispersion, we construct mock catalogs, and perform simulated observation of mock stars drawn from these catalogs. In this Monte Carlo simulation, each mock catalog is designed so that the distribution of r for the relatively metal-rich (or very metal-poor) mock stars resemble those of the observed relatively metal-rich (or very metal-poor) BHB stars, and that the velocity of the mock stars obey a given anisotropic Gaussian velocity distribution (with or without net rotation). We vary the velocity anisotropy parameter, $\beta = 1 - (\sigma_\theta^2 + \sigma_\phi^2)/(2\sigma_r^2)$, and produce 1000 mock catalogs for each case. We find that the derived σ_θ and σ_ϕ is only reliable for $r < 16$ kpc and $r < 18$ kpc for the relatively metal-rich and very metal-poor sample, respectively, while estimates of σ_r are reliable at any r .

4. APPLICATION OF OUR METHODOLOGY – DERIVATION OF ROTATION VELOCITIES, VELOCITY DISPERSIONS, AND VELOCITY ANISOTROPY PARAMETERS

Throughout this paper, we assume that the Local Standard of Rest (LSR) is on a circular orbit with a rotation speed of 220 km s^{-1} (Kerr & Lynden-Bell 1986). It is worth noting that our assumed values for the Galactocentric distance of the Sun, $R_\odot = 8.5$ kpc, and the circular velocity of the LSR are both consistent with two recent independent determinations of these quantities by Ghez et al. (2008) and Koposov et al. (2010). Bovy et al. (2012) have recently determined, on the basis of accurate line-of-sight velocities for stars in the APOGEE sub-survey of SDSS-III, that the circular velocity of the LSR is close to 220 km s^{-1} . We also assume that the peculiar motion of the Sun with respect to the LSR is $(U_\odot, V_\odot, W_\odot) = (10.0, 5.3, 7.2) \text{ km s}^{-1}$ (Dehnen & Binney 1998).

Figure 1 shows the determination of mean rotational velocity, V_{rot} , for the relatively metal-rich (red) and very metal-poor (blue) BHB samples, as a function of Galactocentric distance, r . The shaded regions indicate the uncertainties in each result, estimated from a bootstrap approach (sampling with replacement). Inspection of this figure suggests that V_{rot} at $13\text{--}23$ kpc is a slightly decreasing function of r for the relatively metal-rich sample, while that for the very metal-poor sample is more or less flat. The relatively more metal-rich sample is in modest prograde rotation, with $V_{\text{rot}} \sim 0\text{--}20 \text{ km s}^{-1}$, while the very metal-poor sample is in retrograde motion, with $V_{\text{rot}} \sim -20$ to -50 km s^{-1} , and lags that of the relatively metal-rich sample by $\sim 20\text{--}50 \text{ km s}^{-1}$, similar to previous observations of stars in a much more local sample by Carollo et al. (2007, 2010), the outer-halo analysis based on distribution-function fitting (Deason et al. 2011), and some recently simulated stellar haloes (e.g., Tissera et al. 2012). It is also intriguing to see that the rotational shear between two samples seems to shrink at $r \sim 20$ kpc. We confirm that varying the LSR velocity only changes the absolute value of V_{rot} , and that the very metal-poor sample *always* lags behind the relatively metal-rich sample, independent of the assumed LSR velocity.

Figure 2 shows determinations of the radial velocity dispersion, σ_r , and the two components of the tangential velocity dispersion, σ_θ and σ_ϕ , for the relatively metal-rich and very metal-poor samples, as a function of r . As seen in the figure, σ_r is about 100 km s^{-1} , and exhibits a declining behavior over $12.5 < r < 20$ kpc for both samples, supporting most previous studies (e.g., Xue et al. 2008; Brown et al. 2010). In

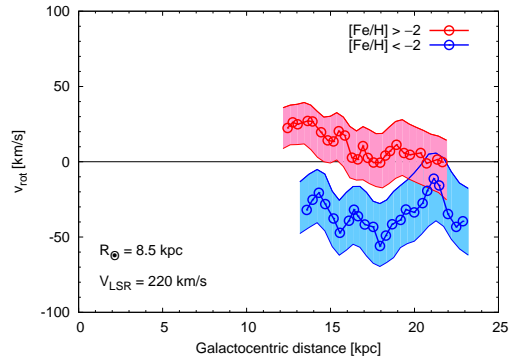


FIG. 1.— The mean rotational velocity, V_{rot} , for the relatively metal-rich BHB sample (red) and very metal-poor BHB samples (blue), as a function of Galactocentric distance r . Open circles show the result for our BHB samples. In this plot, we bin the relatively metal-rich (and very metal-poor) BHB stars in r by binning 500 stars (400 stars), sorted in r , and moving through the sample in steps of 20 stars. Each bin contains stars with a typical standard deviation in r of ~ 3 kpc, and the resultant V_{rot} is presented at the median value of r . The associated shaded regions represent the uncertainties of our results, estimated from the bootstrap method, and denote the range covered by the 16% and 84% percentiles.

addition, this figure suggests that $\sigma_\theta \simeq \sigma_\phi$ holds for the very metal-poor sample. Noting that the gravitational potential is nearly spherical well above the disk plane, and that V_{rot} of the very metal-poor stars is small compared with its velocity dispersion, it follows that they obey a distribution function that depends mainly on the orbital energy and angular momentum (Binney & Tremaine 2008), and thus their spatial distribution is nearly spherical. The different behavior of the 3D velocity dispersions for the two samples implies that both the functional form of the distribution function and spatial distribution for these samples are different.

Figure 3 shows the velocity anisotropy parameter, $\beta = 1 - (\sigma_\theta^2 + \sigma_\phi^2)/(2\sigma_r^2)$. This parameter quantifies the relative dominance of the radial and tangential velocity dispersions, and provides a simple diagnostic of the orbital properties of our sample stars. If β takes on values $\beta < 0$, we can infer that the halo stars are dominated by round orbits, while if $0 < \beta < 1$, we can infer that the halo stars are dominated by radial orbits. When β is (nearly) zero, we can infer that the velocity distribution is (nearly) isotropic. Figure 3 suggests that relatively metal-rich BHB stars are dominated by radial orbits at $12 < r/\text{kpc} < 15$ ($\beta = 0.3 \pm 0.3$), while the very metal-poor BHB stars are dominated by circular orbits over $13 < r/\text{kpc} < 18$ ($\beta = -0.9 \pm 0.7$). A similar trend in the eccentricity distribution is also confirmed in the more local sample of halo stars reported by Carollo et al. (2010), in which very metal-poor halo stars possess a higher fraction of low-eccentricity orbits (see their Figure 5).

5. DISCUSSION AND CONCLUSIONS

The observed systematic differences in the orbital motions of the relatively metal-rich and very metal-poor BHB stars suggest that the orbital motion of the progenitor systems of the stellar halo depends on their metal abundances. Noting that dwarf galaxies with smaller total stellar masses tend to have lower metal abundances (Kirby et al. 2008, and references therein), which can be understood as a result of a smaller rate of metal-enrichment events such as supernova explosions, our findings suggest that low-gas-fraction (‘star-rich’) systems tend to move in radial orbits, while high-gas-fraction (‘gas-rich’) systems tend to move in round orbits when they

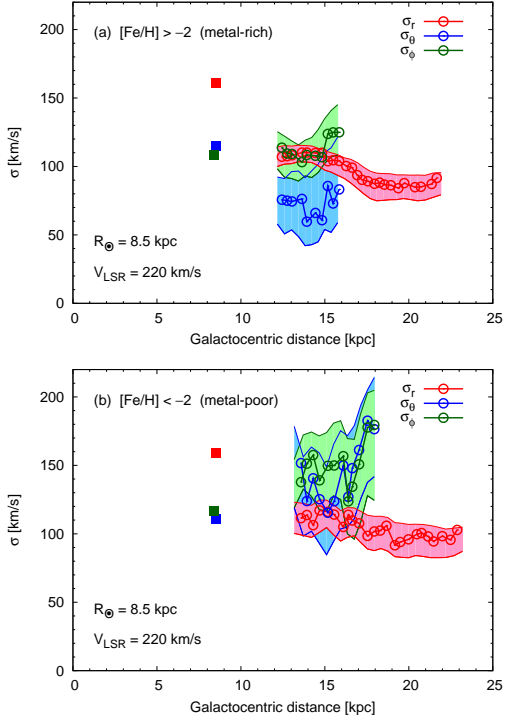


FIG. 2.— Three-dimensional velocity dispersions σ_r (red), σ_θ (blue), and σ_ϕ (green), as a function of Galactocentric distance. Open circles show the result for our BHB samples. The same binning procedure as in Figure 1 is adopted. For the tangential velocity dispersions, some of the bins with large Galactocentric distance are excluded, because of a large systematic error indicated from Monte Carlo simulations. The associated shaded regions represent the uncertainties of our results, estimated from the bootstrap method. Results for the relatively metal-rich BHB sample and very metal-poor BHB sample are shown in panel (a) and (b), respectively. Filled squares at $r = 8.5$ kpc in panel (a) and (b) represent the Solar-neighborhood observations of halo stars with $-2 < [\text{Fe}/\text{H}] < -1.6$ and $[\text{Fe}/\text{H}] < -2$, respectively, taken from Chiba & Yoshii (1998).

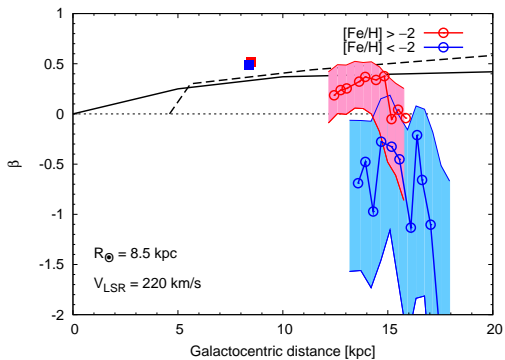


FIG. 3.— The velocity anisotropy parameter, $\beta = 1 - (\sigma_\theta^2 + \sigma_\phi^2) / (2\sigma_r^2)$, for the relatively metal-rich (red) and very metal-poor (blue) BHB samples, as a function of Galactocentric distance. Open circles show the result for our BHB samples, and correspond to those bins presented in Figure 2. The associated shaded regions represent the uncertainties of our results, estimated from the bootstrap method. Filled squares at $r = 8.5$ kpc represent the Solar-neighborhood observations of halo stars with $-2 < [\text{Fe}/\text{H}] < -1.6$ (red) and $[\text{Fe}/\text{H}] < -2$ (blue), taken from Chiba & Yoshii (1998). The black solid and black dashed line represent the β profiles of simulated stellar haloes from Diemand et al. (2005) and Sales et al. (2007), respectively. The dotted horizontal line at $\beta = 0$ is added to guide the eye.

convert their gas to stars.

In the hierarchical galaxy formation scenario, the Milky Way (and other large systems) attains its mass as a result of the mergers of infalling smaller systems (White & Rees 1978; Blumenthal et al. 1984). Due to the deep gravitational potential well of the Milky Way, these infalling systems tend to have radial orbits (Sales et al. 2007). At this stage, we expect that the orbital properties of infalling systems is independent of whether they are star-rich or gas-rich. However, the situation may be different when such radially infalling systems pass near the Galactic center. In such a region, star-rich systems (e.g., massive dwarf galaxies with low gas fractions) are expected to be disrupted by tidal interactions, which give rise to field halo stars with radial orbits (Sales et al. 2007). On the other hand, gas-rich systems are expected to interact with other gas-rich systems, and lose some orbital energy via dissipational processes (Sommer-Larsen & Christensen 1989; Theis 1996; Sharma et al. 2012). If the angular momentum of such a gas-rich system is approximately conserved, the orbit is circularized, and the pericentric distance (distance of closest approach to the Galactic center) increases. Once its pericentric distance become sufficiently large to avoid the central region of the Milky Way, further orbital change becomes less likely, since encounters with other gas-rich systems becomes less probable. Therefore, gas-rich systems tend to move in round orbits. When the Galactic disk forms, some gas-rich systems with similar orbital motions to disk gas may be absorbed into the disk, due to their small relative velocities, while others remain moving on orbits across the halo, and eventually form field halo stars with round orbits. If the total orbital angular momentum of gaseous systems is initially near zero, these halo stars would exhibit a net retrograde rotation with respect to disk stars. Some gas-rich systems in the Milky Way that have not yet formed many stars might be associated with the observed high-velocity clouds (Blitz et al. 1999; Putman et al. 2012).

In the Solar neighborhood, observations suggest that $\beta \simeq 0.5$ for halo stars, almost independent of metal abundance (Chiba & Yoshii 1998; see also Yoshii & Saio 1979), as overplotted in Figure 3. Combined with our result, we see that the motion of the relatively metal-rich BHB stars move on radial orbits at $8.5 < r/\text{kpc} < 15$. This behavior is consistent with recent cosmological simulations in which most halo stars originate from accreted dwarf galaxies (Diemand et al. 2005; Sales et al. 2007), as also overplotted in Figure 3. However, our very metal-poor halo BHB stars suggest a transition from radially-anisotropic to tangentially-anisotropic velocity distributions. The existence of very metal-poor outer-halo stars with round orbits, which is not confirmed in simulated stellar haloes, suggests that current simulations of disk galaxy formation may lack some important mechanisms, such as those proposed in the previous paragraph. We here note that many authors have pointed out that the simulated dwarf galaxies show an over-production of stars, when compared with observed dwarf galaxies (Sawala et al. 2011). This phenomenon is often called the “overcooling problem”, and this might result in underestimation of the gas-rich progenitors in simulated haloes, which in turn underestimate the numbers of metal-poor halo stars with round orbits.

We find that the kinematics of outer-halo stars exhibit a marked dependence on stellar metal abundance, which provides information about the physical properties of their progenitor systems (such as the gas fraction). Both of our main results, that the relatively metal-rich and very metal-poor stars

are dominated by radial and round orbits, respectively, and that the mean rotational velocity of very metal-poor halo stars lags that of relatively metal-rich halo stars, can be explained if very metal-poor stars originate from gas-rich systems and metal-rich stars from star-rich systems. Our findings cast a new light on the formation mechanism of the Milky Way and

similar disk galaxies.

We thank Naoto Kobayashi, Tsuyoshi Sakamoto, and Shigeki Inoue for useful discussions. KH is supported by JSPS Research Fellowship for Young Scientists (23-954). TCB and YSL acknowledge partial support for this work from PHY 02-16783 and PHY 08-22648: Physics Frontiers Center / JINA, awarded by the US National Science Foundation.

REFERENCES

- Aihara, H., Allende Prieto, C., An, D., et al. 2011, *ApJS*, 193, 29
- Binney, J., & Tremaine, S. 2008, *Galactic Dynamics: Second Edition*, by James Binney and Scott Tremaine. ISBN 978-0-691-13026-2 (HB). Published by Princeton University Press, Princeton, NJ USA, 2008.
- Blitz, L., Spergel, D. N., Teuben, P. J., Hartmann, D., & Burton, W. B. 1999, *ApJ*, 514, 818
- Blumenthal, G. R., Faber, S. M., Primack, J. R., & Rees, M. J. 1984, *Nature*, 311, 517
- Bovy, J., Allende Prieto, C., Beers, T. C., et al. 2012, *ApJ*, 759, 131
- Brown, W. R., Geller, M. J., Kenyon, S. J., & Diaferio, A. 2010, *AJ*, 139, 59
- Carollo, D., Beers, T. C., Lee, Y. S., et al. 2007, *Nature*, 450, 1020
- Carollo, D., Beers, T. C., Chiba, M., et al. 2010, *ApJ*, 712, 692
- Chiba, M., & Yoshii, Y. 1998, *AJ*, 115, 168
- Chiba, M., & Beers, T. C. 2000, *AJ*, 119, 2843
- Deason, A. J., Belokurov, V., & Evans, N. W. 2011, *MNRAS*, 411, 1480
- Deason, A. J., Belokurov, V., Evans, N. W., & An, J. 2012, *MNRAS*, 424, L44
- Dehnen, W., & Binney, J. J. 1998, *MNRAS*, 298, 387
- Diemand, J., Madau, P., & Moore, B. 2005, *MNRAS*, 364, 367
- Frenk, C. S., & White, S. D. M. 1980, *MNRAS*, 193, 295
- Ghez, A. M., Salim, S., Weinberg, N. N., et al. 2008, *ApJ*, 689, 1044
- Kafle, P. R., Sharma, S., Lewis, G. F., & Bland-Hawthorn, J. 2012, *ApJ*, 761, 98
- Kerr, F. J., & Lynden-Bell, D. 1986, *MNRAS*, 221, 1023
- Kinman, T. D., Cacciari, C., Bragaglia, A., Smart, R., & Spagna, A. 2012, *MNRAS*, 422, 2116
- Kirby, E. N., Simon, J. D., Geha, M., Guhathakurta, P., & Frebel, A. 2008, *ApJ*, 685, L43
- Koposov, S. E., Rix, H.-W., & Hogg, D. W. 2010, *ApJ*, 712, 260
- Lee, Y. S., Beers, T. C., Sivarani, T., et al. 2008, *AJ*, 136, 2022
- McCarthy, I. G., Font, A. S., Crain, R. A., et al. 2012, *MNRAS*, 420, 2245
- Morrison, H. L., Flynn, C., & Freeman, K. C. 1990, *AJ*, 100, 1191
- Putman, M. E., Peek, J. E. G., & Jounge, M. R. 2012, *ARA&A*, 50, 491
- Sales, L. V., Navarro, J. F., Abadi, M. G., & Steinmetz, M. 2007, *MNRAS*, 379, 1464
- Sawala, T., Guo, Q., Scannapieco, C., Jenkins, A., & White, S. 2011, *MNRAS*, 413, 659
- Sharma, S., Steinmetz, M., & Bland-Hawthorn, J. 2012, *ApJ*, 750, 107
- Sirko, E., Goodman, J., Knapp, G. R., et al. 2004, *AJ*, 127, 914
- Sommer-Larsen, J., Beers, T. C., Flynn, C., Wilhelm, R., & Christensen, P. R. 1997, *ApJ*, 481, 775
- Sommer-Larsen, J., & Christensen, P. R. 1989, *MNRAS*, 239, 441
- Theis, C. 1996, *The History of the Milky Way and Its Satellite System*, 112, 35
- Thom, C., Flynn, C., Bessell, M. S., et al. 2005, *MNRAS*, 360, 354
- Tissera, P. B., White, S. D. M., & Scannapieco, C. 2012, *MNRAS*, 420, 255
- White, S. D. M., & Rees, M. J. 1978, *MNRAS*, 183, 341
- Wilhelm, R., Beers, T. C., & Gray, R. O. 1999, *AJ*, 117, 2308
- Woolley, R. 1978, *MNRAS*, 184, 311
- Xue, X. X., Rix, H. W., Zhao, G., et al. 2008, *ApJ*, 684, 1143
- Xue, X.-X., Rix, H.-W., Yanny, B., et al. 2011, *ApJ*, 738, 79
- Yoshii, Y., & Saio, H. 1979, *PASJ*, 31, 339